Magn Reson Med Sci 2023; 22; 289–300
doi:10.2463/mrms.mp.2020-0123 Published Online: May 10, 2022

MAJOR PAPER

The Utility of Arterial Transit Time Measurement for Evaluating the Hemodynamic Perfusion State of Patients with Chronic Cerebrovascular Stenosis or Occlusive Disease: Correlative Study between MR Imaging and ^{15}O-labeled H_2O Positron Emission Tomography

Kayo Takeuchi[1*], Makoto Isozaki[2], Yoshifumi Higashino[2], Nobuyuki Kosaka[1], Ken-ichiro Kikuta[2], Shota Ishida[3], Masayuki Kanamoto[3], Naoyuki Takei[4], Hidehiko Okazawa[5], and Hirohiko Kimura[1]

Purpose: To verify whether arterial transit time (ATT) mapping can correct arterial spin labeling-cerebral blood flow (ASL-CBF) values and to verify whether ATT is a parameter that correlates with positron emission tomography (PET)-oxygen extraction fraction (OEF) and PET-mean transit time (MTT).

Methods: Eleven patients with unilateral major cerebral artery stenosis or occlusion underwent MRI and PET in the chronic or asymptomatic phase. ASL-MRI acquisitions were conducted with each of two post-label delay (PLD) settings (0.7s and 2.0s) using a pseudo-continuous ASL pulse sequence and 3D-spin echo spiral readout with vascular crusher gradient. ATT maps were obtained using a low-resolution pre-scan approach with five PLD settings. Using the ASL perfusion images and ATT mapping, ATT-corrected ASL-CBF images were obtained. Four kinds of ASL-CBF methods (PLD 0.7s with or without ATT correction and PLD 2.0s with or without ATT correction) were compared to PET-CBF, using vascular territory ROIs. ATT and OEF were compared for all ROIs, unaffected side ROIs, and affected side ROIs, respectively. ATT and MTT were compared by the ratio of the affected side to the unaffected side. Transit time-based ROIs were used for the comparison with ATT.

Results: Comparing ASL-CBF and PET-CBF, the correlation was higher with ATT correction than without correction, and for a PLD of 2.0s compared with 0.7s. The best correlation was for PLD of 2.0s with ATT correction ($R^2 = 0.547$). ROIs on the affected side showed a low but significant correlation between ATT and PET-OEF ($R^2 = 0.141$). There was a low correlation between the ATT ratio and the MTT ratio ($R^2 = 0.133$).

Conclusion: Low-resolution ATT correction may increase the accuracy of ASL-CBF measurements in patients with unilateral major cerebral artery stenosis or occlusion. In addition, ATT itself might have a potential role in detecting compromised hemodynamic state.

Keywords: *arterial spin labeling, arterial transit time, magnetic resonance imaging, cerebral blood flow, oxygen extraction fraction*

Introduction

Arterial spin labeling (ASL) is a technique for assessing cerebral blood flow (CBF) by MRI using magnetically labeled blood as an endogenous tracer by inverting the spin of blood in the cervical vessels through RF irradiation of the cervical vessel level for a certain period of time.[1–3] Due to its non-invasiveness and concurrent accessibility to morphological

[1]Department of Radiology, Faculty of Medical Sciences, University of Fukui, Yoshida-gun, Fukui, Japan
[2]Department of Neurosurgery, Faculty of Medical Sciences, University of Fukui, Yoshida-gun, Fukui, Japan
[3]Radiological Center, University of Fukui Hospital, Yoshida-gun, Fukui, Japan
[4]Global MR Applications and Workflow, GE Healthcare, Tokyo, Japan
[5]Biomedical Imaging Research Center, University of Fukui, Yoshida-gun, Fukui, Japan
*Corresponding author: Department of Radiology, Faculty of Medical Science, University of Fukui, 23-3, Matsuokashimoaizuki, Eiheiji-cho, Yoshida-gun, Fukui 910-1193, Japan. Phone: +81-776-61-8371, Fax: +81-776-61-8137, E-mail: takek@u-fukui.ac.jp

Received: September 4, 2020 | Accepted: February 7, 2022

information, ASL has been applied to imaging in various central nervous system disorders, including acute[4] and chronic cerebrovascular disorders,[5] brain tumors,[6,7] epilepsy,[8] and shunt disorders.[9,10]

Whereas ASL allows simple CBF measurement, underestimation of CBF in patients with chronic main artery stenosis or occlusion is a problem.[11] In pseudo-continuous ASL imaging, the period of RF irradiation and the time between the end of irradiation and image acquisition are defined as the labeling duration (LD) and post-label delay (PLD), respectively. The time taken for the inverted spins to travel from the cervical vessel to the brain parenchyma is called the arterial transit time (ATT). In patients with chronic main artery stenosis or occlusion, heterogeneous prolonged ATT due to collateral pathways results in underestimation of regional CBF with single PLD acquisition.[11] The simplest method is the use of long PLD to reduce the sensitivity of ATT to CBF measurement, but the use of longer PLD does not necessarily provide a sufficient SNR because the longer the PLD, the more the labeling effect is lost.[3]

The clinical evaluation of patients with chronic main artery stenosis or occlusion is currently performed using both morphological assessment by MRI and functional assessment by positron emission tomography (PET) (or single photon emission computed tomography [SPECT]). These patients are divided into three stages (0–2) proposed by Powers.[12] The group of patients with severe cerebral circulatory disturbance and an extremely high recurrence rate of cerebral infarction corresponds to stage 2, misery perfusion, which can be detected by decreased CBF, increased oxygen extraction fraction (OEF), and prolongation of mean transit time (MTT) measured by PET. The detection and treatment of this high-risk group is crucial to improve their prognosis.[13,14] Whereas PET is useful for functional evaluation, it has limited availability, higher cost, and greater radiation exposure when compared to MRI. Therefore, it would be clinically very useful if MRI could be used to accurately measure CBF and to measure biomarkers of hemodynamic cerebral ischemia instead of OEF and MTT.

Thus, we decided to make the following two assessments in the present study. The first one assessment deals with accurate CBF measurement. When a quantitative CBF value from ASL is preferred, extended scan time is necessary to measure additional physiological parameters, such as the T1 of brain tissue, T1 of arterial blood, arterial blood volume, and ATT.[15] Of the parameters required to measure absolute CBF by ASL, ATT is the most crucial, especially in patients with occlusive cerebrovascular disease.[11,16] Several methods to improve the quantification of ASL-CBF have been reported,[3,17] and the most straightforward approach is to acquire ASL images with multiple consecutive PLDs.[18,19] In fact, a more accurate ATT-corrected CBF map can be reportedly obtained based on multi-PLD ASL acquisition data than on single PLD.[16] However, since ASL has a low SNR and a long acquisition time, such a simple multiple-PLD approach is difficult to use in routine clinical examinations. As a solution, the combination of a low-resolution ATT preparation scan and a high-resolution scan with a long LD enables an ATT-corrected CBF map to be obtained within a feasible time frame in the clinical setting.[20] Whether reliable CBF measurements could be obtained with this method was examined.

The second assessment is whether there are MRI parameters from ASL acquisition that can be used as an alternative to OEF or MTT. It has been reported that ATT is prolonged in the territory of a stenotic vessel, and that prolongation of ATT itself may indicate hemodynamic ischemia.[21,22] In this study, whether ATT could be a surrogate index for assessing hemodynamic cerebral ischemia instead of OEF or MTT obtained from PET was investigated.

Thus, the aims of this study were to: 1) verify whether low-resolution ATT mapping can correct single PLD ASL-CBF, and 2) evaluate whether ATT may play a role as a surrogate measure of hemodynamics, especially in relation to PET-OEF and PET-MTT.

Materials and Methods

Patients

The analysis was performed using data collected in a prospective registry of patients with cerebral artery stenosis and occlusion who visited our hospital; this registry was continuously operated from January 2014 to September 2015. The inclusion criteria were as follows: (1) internal carotid artery (ICA) and middle cerebral artery (MCA) stenosis or occlusion diagnosed morphologically (ultrasound sonography or MR angiography and digital subtraction angiography [DSA]); (2) at least 1 month had passed after an event such as hemiparesis or dysarthria or in the asymptomatic (chronic) phase; and (3) age between 20 and 85 years. The exclusion criteria were as follows: (1) contraindications to MRI; (2) inability to consent to participate in this study; and (3) bilateral lesions. Thirteen patients fulfilled the inclusion criteria, but two of them were excluded due to bilateral lesions. This prospective study was approved by our hospital's Institutional Ethics Committee, and informed consent was obtained from all the patients.

All the patients underwent both MRI and PET, and the interval between MRI and PET was within 2 months. The data of 11 patients were analyzed (eight men: median age, 66 years; age range, 26–73 years; and three women: median age, 45 years; age range, 43–69 years). The clinical characteristics of the study population are summarized in Table 1. According to the Powers stage classification,[12] 4 of the 11 patients were in stage II. The stenosis ratio was determined by applying the North American Symptomatic Carotid Endarterectomy Trial (NASCET) criteria to cerebral and cervical vessels, a method originally used for evaluating cervical blood vessels. The ratio of stenosis was calculated by the ratio relative to the normal diameter in the vicinity by DSA.[23] In the case of obstruction, the stenosis ratio was set to 100%. This prospective study was approved by our hospital's Institutional Ethics Committee, and informed consent was obtained from all the patients.

Table 1 Patients' characteristics and clinical data

Patient no.	Age (years)/Sex	Angiographic findings (DSA)	Stenosis (%)	stage	Symptom
1	57/M	R MCA occlusion	100	I	Hemiparesis, Dysarthria
2	43/F	R MCA occlusion	100	I	Hemipalegia, Dysarthria
3	66/M	R ICA occlusion	100	I	Hemiplegia
4	69/F	R ICA occlusion	100	I	Asymptomatic
5	71/M	L ICA occlusion	100	I	Aphasia
6	73/M	R ICA stenosis	80	I	Dysarthria
7	66/M	L ICA stenosis	84	I	Hemiplegia, Aphasia
8	73/M	R ICA stenosis	86	I	Asymptomatic
9	45/F	L ICA occlusion	100	I	Asymptomatic
10	56/M	R MCA occlusion	100	0- I	Asymptomatic
11	26/M	R MCA occlusion	100	I	Asymptomatic

DSA, digital subtraction angiography; ICA, internal carotid artery; L, left; MCA, middle cerebral artery; R, right.

ASL

MRI was performed using a 3.0 T whole body scanner (Discovery MR 750; GE Healthcare, Waukesha, WI, USA) and 32-channel head coil. All images were acquired using a pseudo-continuous ASL pulse sequence with 3D-spin echo spiral readout and vascular crusher gradient.[17] ASL-CBF images with two different PLD settings (0.7s and 2.0s) and a low-resolution ASL acquisition for ATT calculation were acquired, and ATT-corrected ASL-CBF images were calculated using ASL-CBF and low-resolution ATT images.[20] The common imaging parameters of ASL-CBF were as follows: LD 4.0s, spiral imaging (512 points × 7 arms), FOV 240 mm, and whole brain with 38–40 slices. Each imaging parameter for ASL-CBF with two different PLDs was as follows: 1) for ASL-CBF with PLD 0.7s, TR 6202 ms, TE 23 ms, and acquisition time 3.5 min; 2) for ASL-CBF with PLD 2.0s, TR 7502 ms, TE 23 ms, and acquisition time 4.5 min.

ATT was measured using a low-resolution (640 × 2 arms) pre-scan approach with five PLDs (0.70, 1.26, 1.85, 2.43, 3.0s, and acquisition time 2.5 min), based on previously reported methods,[20] and an ATT map was created. The total acquisition time to obtain the ATT-corrected ASL-CBF image is the sum of the ASL-CBF and the low-resolution ATT acquisition time, as follows: 6 min with PLD 0.7s and 7 min with PLD 2.0s.

ATT was calculated using the signal-weighted delay (WD) method from equations (1) and (2), using all low-resolution pre-scan acquisition signals,[24] in which model the ASL signal function is converted to a monotonically increasing function for δ_a.[17]

$$WD(\delta_a) = \left(\sum_{i=1}^{n} w_i \cdot \Delta M[\delta_a, w_i]\right) / \left(\sum_{i=1}^{n} \Delta M[\delta_a, w_i]\right) \quad (1)$$

The single-compartment model was assumed for the perfusion signal in WD (Eq. 1).[15]

$$\Delta M(t) = 0 \ (t < \delta_a) \quad (2\text{-}1)$$

$$\Delta M(t) = 2M_0 \alpha T_{1a} f \cdot \left(exp\left[\frac{-\delta_a}{T_{1a}}\right] - exp\left[\frac{-t}{T_{1a}}\right]\right) \ (\delta_a < t < \delta_a + \tau) \quad (2\text{-}2)$$

$$\Delta M(t) = 2M_0 \alpha T_{1a} f \cdot exp\left(\frac{-t}{T_{1a}}\right) \cdot \left(exp\left[\frac{\tau}{T_{1a}}\right] - 1\right) \ (\delta_a + \tau < t) \quad (2\text{-}3)$$

In the above equations, ΔM is the perfusion signal, δ_a is the arterial transit time, w_i is the post-labeling delay of the i-th low-resolution pre-scan acquisition, M0 is the equilibrium magnetization of arterial blood, a is the labeling efficiency (0.85), f is CBF, T_{1a} is the longitudinal relaxation time of arterial blood (1.65s), and τ is the labeling duration.

CBF with ATT correction was calculated from long-labeled, high-resolution ASL data using equation 2 with δ_a values on a pixel-by-pixel basis.

PET

A whole-body PET scanner (Advance; GE Healthcare) was used for PET data acquisition. The scanner permits simultaneous acquisition of 35 image slices in 2D mode with inter-slice spacing of 4.25 mm.[25] Performance tests showed the intrinsic resolution of the scanner to be 4.6–5.7 mm in the transaxial direction and 4.0–5.3 mm in the axial direction. The PET data were reconstructed using a Hanning filter with

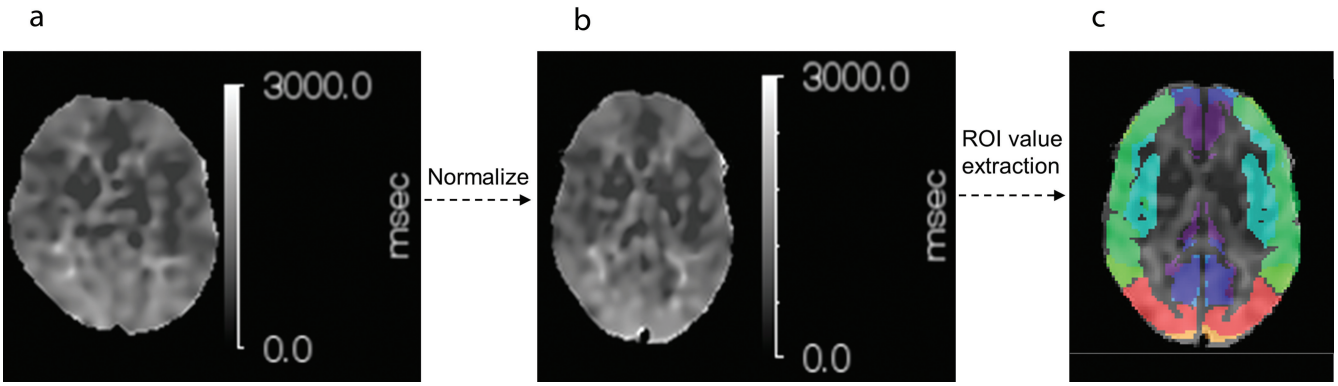

Fig. 1 Sample images of ATT transformation to normalization space. (**a**) ATT, (**b**) normalized ATT, (**c**) fused transit time-based ROI on normalized ATT. (**b**) is a standardized image of (**a**). The ROI is detected by fusing it on a transit time-based ROI. The transit time-based ROI is shown in Fig. 2b. ATT, arterial transit time.

a resolution of 6.0 mm full-width at half-maximum in the transaxial direction. The patients were positioned on the scanner bed with their head immobilized using a head holder. A 10-min transmission scan was acquired before the emission scan with a 68 Ge/68 Ga rod source for attenuation correction. $C^{15}O$ and $^{15}O_2$ inhalation studies were performed to measure cerebral blood volume (CBV) and OEF, respectively. CBF (ml/100 g/min) was then measured with a bolus injection of 740 MBq ^{15}O-water. Radioactivity was counted in frequent sampling of arterial blood during $^{15}O^2$ and $H_2{}^{15}O$ scans. CBF images were calculated from the dynamic PET data and arterial input functions measured from arterial counts using the autoradiographic method.[26] A partition coefficient of 0.9 for ^{15}O-water was used in the CBF calculation. Details of the study protocol have been described previously.[27,28] MTT was calculated from MTT = CBV/CBF based on central volume theory,[29] instead of by the pixel-by-pixel MTT map, and the CBV and CBF values were the mean values of each ROI. A description of the ROI is given in the following paragraph in the data analysis subsection.

Data analysis

All MRI and PET images were reviewed for suitability for analysis based on the consensus opinion of two radiologists (KT with 10 years of experience and HK with 30 years of experience). For objective and reproducible comparisons, all parametric images, such as ASL-CBF, ATT, PET-CBF, OEF, and CBV, were converted to the standardized brain as shown in Fig. 1, and each ROI value was extracted from those standardized images. The MTT of each ROI was calculated from the average CBF and CBV values extracted from standardized space.

Standardized brain

The method of conversion to the standardized brain was as follows. After performing co-registration of ASL-CBF and PET-CBF images to the same whole-brain T1 weighted image (T1WI), the T1WI was converted to a standardized image using a built-in the Montreal Neurological Institute (MNI) template of MRI-T1WI by ISSP (built-in module of NEUROFLEXER, Nihon Medi-Physics, Tokyo, Japan). Similarly, after performing co-registration of ATT, OEF, and CBV images to the same whole-brain T1WI, the T1WI was converted to a standardized image using a built-in MNI template of MRI-T1WI by SPM (version 12; The Wellcome Trust Centre for Neuroimaging). Since ISSP could not convert ATT to the standardized brain correctly, SPM was also used.

ROI value extraction

As for ROI value extraction, two types of ROI sets were used: built-in, pre-defined, vascular territory ROI in NEUROFLEXER, and transit time-based ROI as described in the previous report.[30] To compare ASL-CBF and PET-CBF, each ROI value was extracted using NEUROFLEXER automatic ROI detection software.[31] Figure 2a shows the vascular territory ROIs, which were categorized into six regions: the left and right anterior cerebral artery (ACA) regions, the anterior MCA region, and the posterior MCA region.

Transit time-based ROI value extraction was used to compare ATT and PET parametric images, such as CBF, OEF, ATT, and CBV. Figure 2b shows transit time-based ROIs, which were categorized into 18 regions: the left and right proximal, intermediate, and distal regions of each of the major ACA, MCA, and posterior cerebral artery (PCA) territories. It has been previously reported and is available in MNI standard space.[30]

NEUROFLEXER vascular territory ROIs have been used to evaluate CBF in PET or SPECT, and they are designed to cover cortices on CBF maps from PET or SPECT using curvilinear cortical strip ROIs, with less influence of white matter, which has lower blood flow than the cortex. In contrast, transit time-based ROIs completely cover the whole cortical brain region. The former ROIs do not include the watershed region

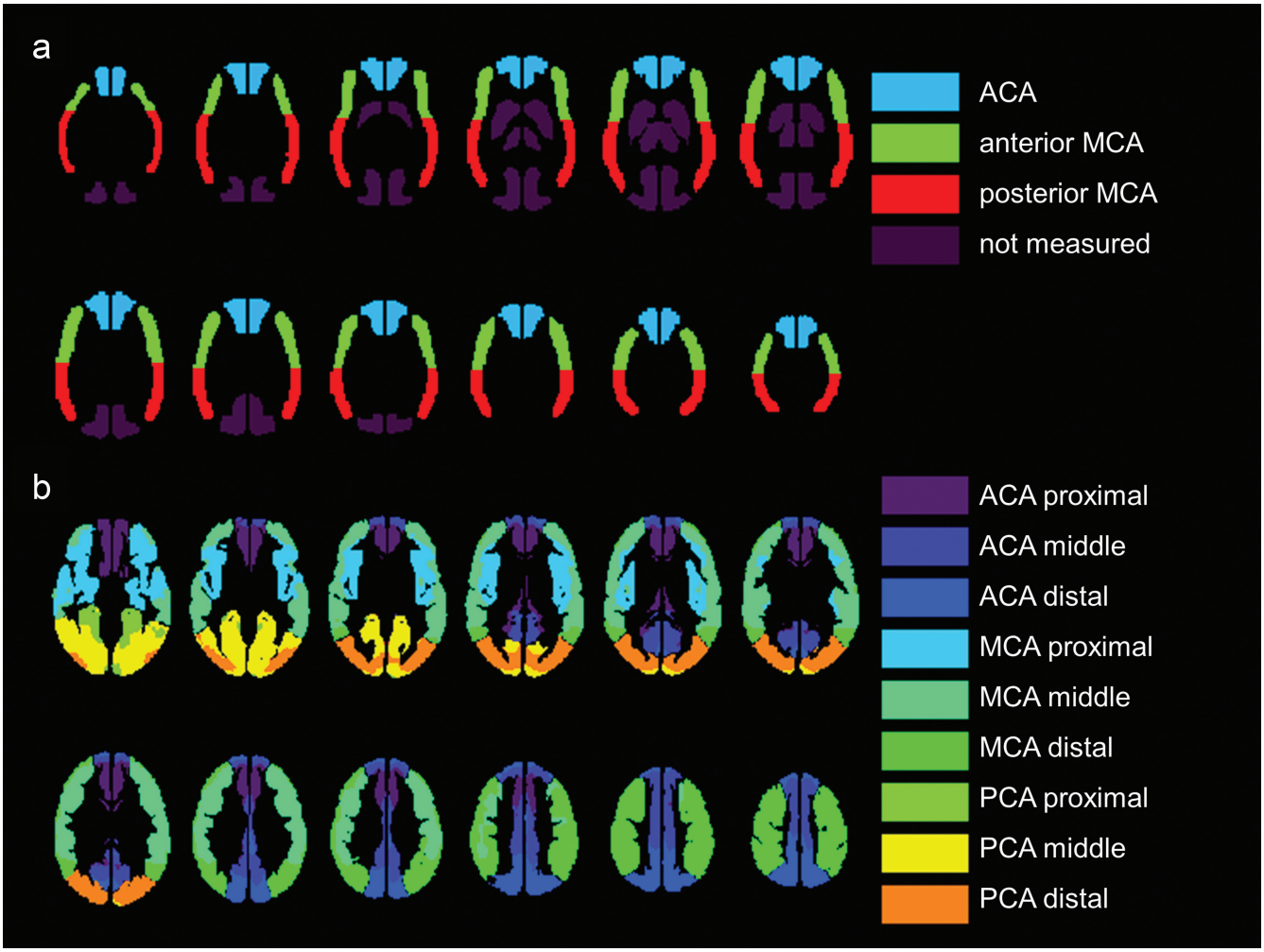

Fig. 2 **a**) Automated ROI detection in the conventional vascular anatomical territories. The ROIs are generated by NEUROFLEXER and cover the major vascular regions. Dark purple regions, including the PCA and basal ganglia, and the thalamus regions are not measured. **b**) Automated ROI detection focusing on the difference in transit time among the major vessel territories. ROIs are set to cover the proximal, middle, and distal regions of the major vascular territories. No measurements are obtained for structures located in the deep gray matter (e.g., the basal ganglia and thalamus). ACA, anterior cerebral artery; MCA, middle cerebral artery; PCA, posterior cerebral artery.

or the high frontal or parietal cortex. However, the transit time-based ROIs include those regions, which correspond to longer transit time regions. Data from these regions are especially important for the assessment of the relationship between ATT and other hemodynamic parameters from PET. In this study, the vascular territory ROIs of NEUROFLEXER were used for CBF, and the transit time-based ROIs were used for ATT. In addition, ATT cannot be analyzed by NEUROFLEXER. OEF and MTT, which were to be compared with ATT, used the same transit time-based ROIs as ATT. MTT in each ROI was calculated from the mean CBF and CBV of PET using the transit time-based ROIs.

Statistical analysis

ASL-CBF and PET-CBF values of the ROIs in both the unaffected and affected sides of each vascular territory were used in the linear regression analyses. The coefficients of correlation between the CBF values obtained in the two modalities were assessed in terms of dependency on the difference in PLD, and with and without ATT correction. Linear regression analysis was also conducted for transit time-based ROIs from ASL-ATT and PET-OEF. In addition, their correlations on the occluded and contralateral unaffected sides were calculated separately.

The regression equation and coefficient of determination were obtained using linear regression analysis with the ROI ASL-CBF of each vascular region as the dependent variable and the PET-CBF value as the independent variable. When the values of ASL-CBF and PET-CBF are exactly the same, the Y-intercept of the regression equation and slope become 0 and 1, respectively. The coefficient of determination, R^2, is considered to have almost negligible correlation when it is 0–0.09, a low

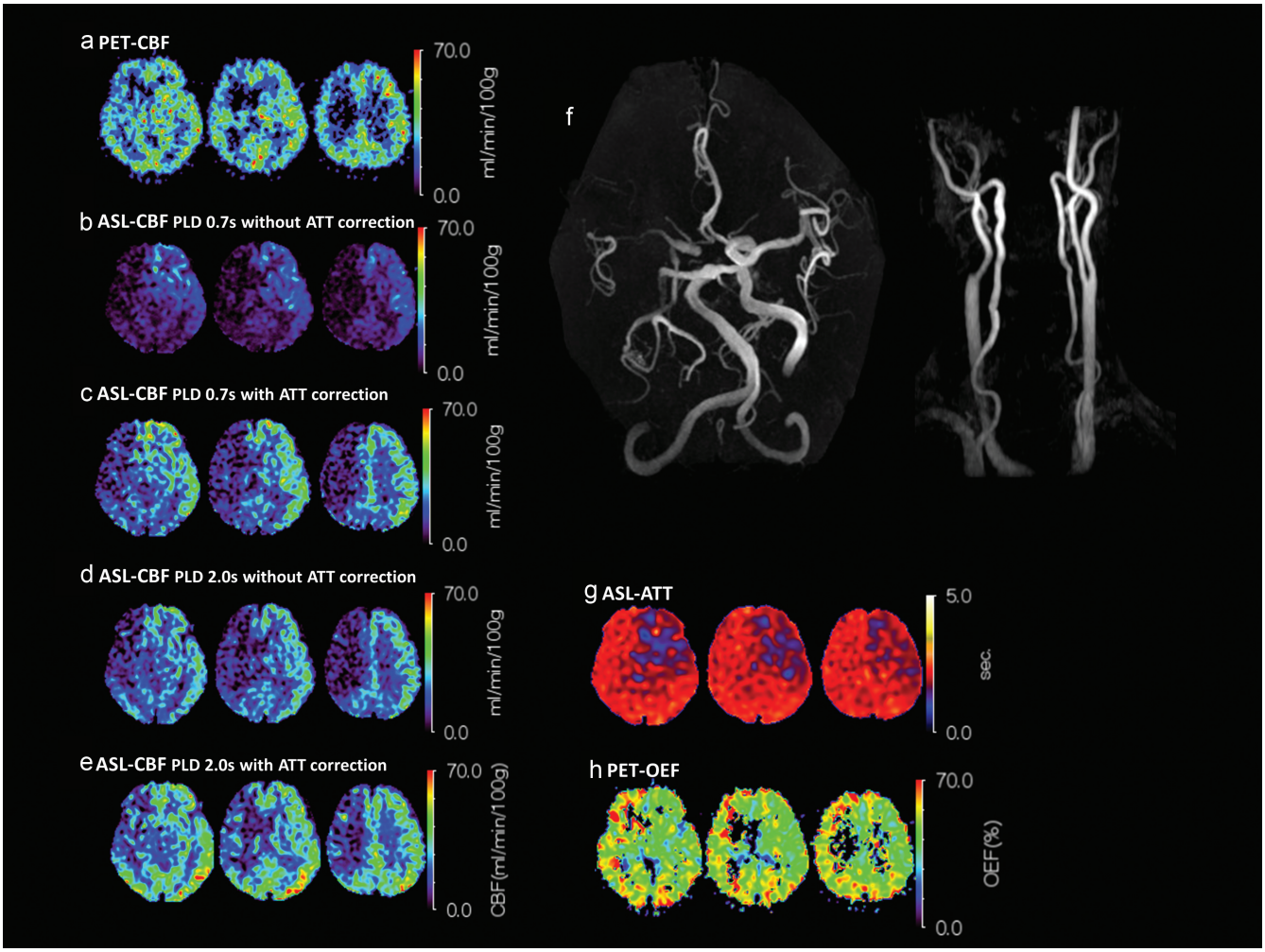

Fig. 3 Representative images of right internal carotid artery occlusion (patient no.3). (**a**) PET-CBF; (**b**) ASL-CBF without ATT correction, PLD = 0.7s; (**c**) ASL-CBF with ATT correction, PLD = 0.7s; (**d**) ASL-CBF without ATT correction, PLD = 2.0s; (**e**) ASL-CBF with ATT correction, PLD = 2.0s; (**f**) MRA-MIP; (**g**) ASL-ATT; (**h**) PET-OEF.Increased OEF (**h**) and prolonged ATT (**g**) areseen in the right MCA territory. Although PET-CBF isslightly decreased in the right MCA territory, the ASL-CBF values are decreased for both PLD times when ATT correction is not used (**b** and **d**). The images for ASL-CBF with longer PLD and with ATT correction (**e**) are the mostsimilar to the PET-CBF images in (**a**). ASL, arterial spin labeling; ATT, arterial transit time; CBF, cerebral blood flow; MCA, middle cerebral artery; MIP, maximum intensity projection; MRA, magnetic resonance angiography; OEF, oxygen extraction fraction; PET, positron emission tomography; PLD, post-label delay.

correlation when it is 0.09–0.25, a moderate correlation when it is 0.25–0.49, and a high correlation when it is 0.49–1.[32] The coefficient of correlation between the CBF values obtained on MRI and PET was evaluated between: 1) ASL-CBF without ATT correction (PLD 0.7s) and PET-CBF; 2) ASL-CBF with ATT correction (PLD 0.7s) and PET-CBF; 3) ASL-CBF without ATT correction (PLD 2.0s) and PET-CBF; and 4) ASL-CBF with ATT correction (PLD 2.0s) and PET-CBF.

A linear regression analysis was also performed with ASL-ATT as the dependent variable and PET-OEF as the independent variable. In addition, correlations between all ROIs, the unaffected side ROIs, and affected side ROIs were also calculated separately.

A linear regression analysis was performed with the ratio between the affected side and the unaffected side of ASL-ATT as the dependent variable and the ratio between the affected side and the unaffected side of PET-MTT as the independent variable.

Results

Figure 3 shows a typical case of occlusion of the right ICA in which the right intracranial ICA and the right MCA territory are fed by the collateral circulation. The PET images demonstrate misery perfusion characterized by increased OEF in the right MCA territory (PET-CBF 27.4 ml/100 g/min, OEF 51.1%). The ASL-CBF map using PLD 0.7s without ATT correction shows a low signal in the right MCA region (3.27 ml/100 g/min) that was 10.3 ml/100 g/min with ATT correction. Furthermore, by setting PLD to 2.0s, it was

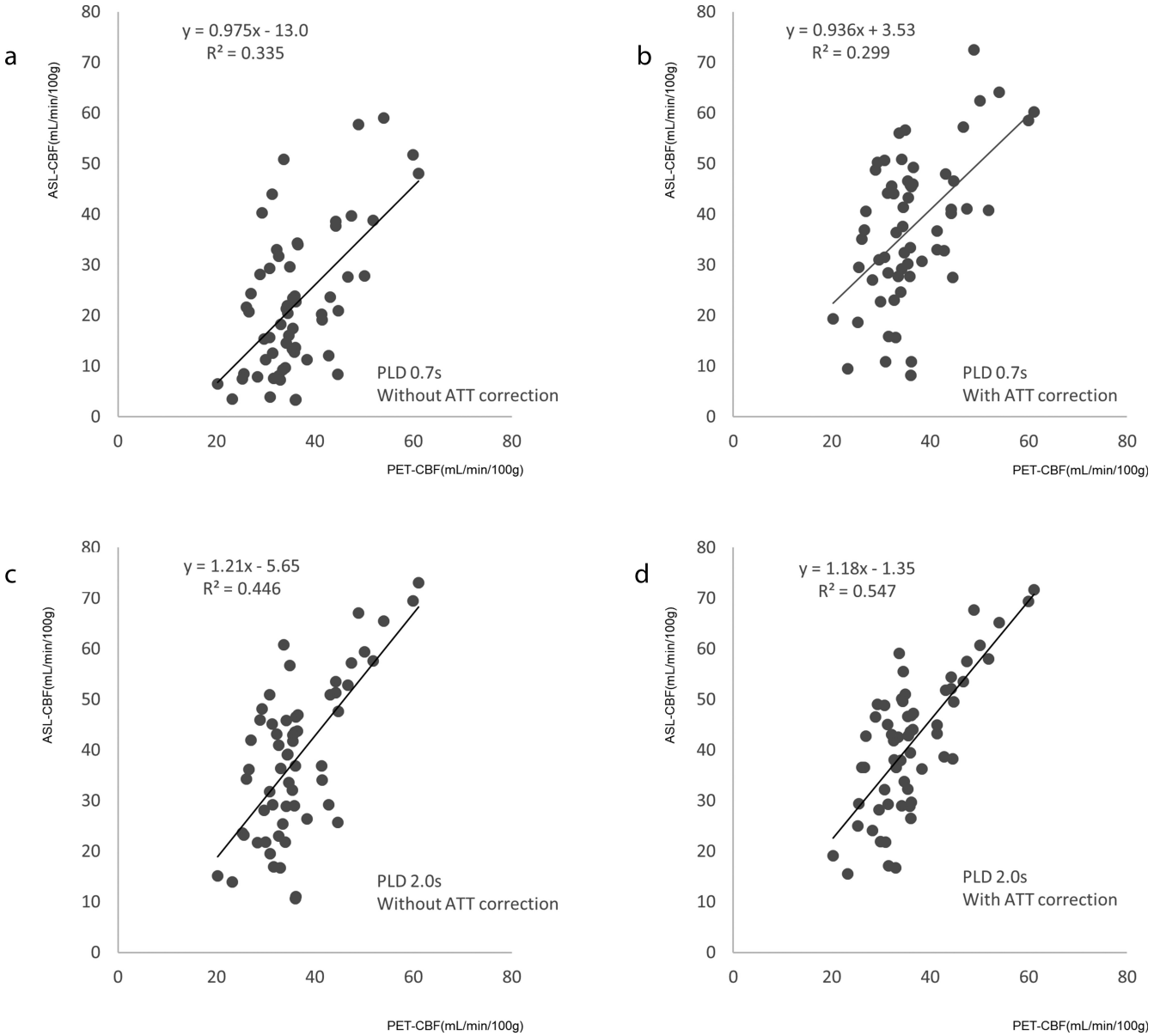

Fig. 4 Comparison between cerebral blood flow measured by MRI and PET for all ROIs. (**a**) PLD = 0.7s without ATT correction, (**b**) PLD = 0.7s with ATT correction, (**c**) PLD = 2.0s without ATT correction, and (**d**) PLD = 2.0s with ATT correction. The regression line and coefficient of determination (R^2) are inset on each graph. The reliability of the ASL-CBF values improves with ATT correction. Among the PLD and ATT correction settings, the best R^2 value is obtained for ASL-CBF with PLD 2.0s and ATT correction. ASL-CBF, arterial spin labeling-cerebral blood flow; ATT, arterial transit time; CBF, cerebral blood flow; PET, positron emission tomography; PLD, post-label delay; R^2, coefficient of determination.

16.4 ml/100 g/min, and finally with ATT correction, it was 18.3 ml/100 g/min, which is closer to the PET-CBF. With longer PLD and ATT correction, the measured ASL-CBF values and the appearance of CBF mapping were correlated with PET-CBF. The mean ATT of the right MCA area was 2133 ms.

Figure 4 shows the comparison between ASL-CBF and PET-CBF for different PLD values and with or without ATT correction in all ROIs. In all the conditions, significant positive correlations were found between ASL-CBF and PET-CBF, and PLD 2.0s with ATT correction (Fig. 4d) showed the best correlation ($R^2 = 0.547$). In PLD 0.7 without ATT correlation (Fig. 4a), most of the ASL-CBF showed lower values compared to the PET-CBF. However, these CBF underestimations were compensated for by ATT correction (Fig. 4b) or the use of the longer PLD 2.0s (Fig. 4c). With PLD 2.0s settings (Fig. 4c and 4d), ATT correction did not substantially increase ASL-CBF, but it improved the correlation between ASL-CBF and PET-CBF.

Table 2 shows correlations between ASL-CBF and PET-CBF in all ROIs, the unaffected side ROIs, and affected side ROIs, respectively. The data for all ROIs was the same as the equation in Fig. 4. On the unaffected side, there was a

Table 2 Correlations between ASL-CBF and PET-CBF for all, unaffected side, and affected side

	PLD	ATT correction	Regression equation		R^2
			Slope	Intercept	
ALL	0.7s	without	0.975	−13.0	0.335
	0.7s	with	0.936	3.53	0.299
	2.0s	without	1.21	−5.65	0.446
	2.0s	with	1.18	−1.35	0.547
Unaffected	0.7s	without	0.745	−0.408	0.218
	0.7s	with	0.406	26.9	0.118
	2.0s	without	0.873	10.7	0.336
	2.0s	with	0.881	12.5	0.447
Affected	0.7s	without	0.970	−16.5	0.378
	0.7s	with	1.37	−14.2	0.418
	2.0s	without	1.37	−14.5	0.487
	2.0s	with	1.38	−10.4	0.599

R^2, the coefficient of determination.

moderate correlation with PLD 2.0s with or without ATT correction. However, when the PLD was 0.7s, the correlation of ASL-CBF on the unaffected side was slightly worse with ATT correction. On the affected side, with PLD 2.0s and ATT correction, the intercept of the regression equation was still lower than 0.

Figure 5 shows scatterplots of the correlation between PET-OEF and ASL-ATT. There is a low but significant correlation of the overall data, as shown in Fig. 5a ($R^2 = 0.095$, $P < 0.05$). There was a negligible correlation of values from the contra-lateral unaffected side, as shown in Fig. 5b ($R^2 = 0.058$, $P = 0.157$). The correlation tended to increase in the regression of data from only the affected brain hemisphere, as shown in Fig. 5c ($R^2 = 0.141$, $P < 0.05$).

The ratio between the affected side and the unaffected side of ATT and the ratio between the unaffected side and the affected side of MTT showed a low correlation: $y = 0.250x + 82.1$, $R^2 = 0.133$, $P < 0.05$ (figure not shown).

Discussion

This study showed that 1) low-resolution ATT correction makes ASL-CBF values closer to PET-CBF values and they correlate better, and 2) there are weak but significant correlations between ATT and OEF and between the ratio of the affected to the unaffected side of ATT and the ratio of MTT.

A low-resolution ATT map was found to increase the accuracy of ASL-CBF in patients with chronic main artery stenosis or occlusion. The highest correlation was obtained by ATT correction using ASL-CBF with PLD 2.0s. In fact, the ATT map in Fig 3g shows an ATT value of more than 2000 msec on the affected side, suggesting that PLD 2.0s data acquisition is at least required to obtain more reliable CBF measurements, even with ATT correction. The total time for ASL-CBF was 7 min, consisting of 2.5 min for ATT pre-scan and 4.5 min for normal resolution ASL acquisition, which is much shorter than the more than 20 min required for high-resolution ATT correction reported by Tsujikawa et al.[16] ASL-CBF on the affected side was compared to PET-CBF, which we consider to be a standard CBF measurement. Although the affected side ASL-CBF was still calculated as a slightly lower CBF value compared to PET-CBF, low-resolution ATT correction can be used as a method to improve the conventional ASL-CBF measurement in patients with chronic cerebral artery stenosis or occlusive diseases. It is useful and practical as a method to improve CBF measurement.

In the present study, a factor that may explain why ASL-CBF was lower than PET-CBF on the affected side may be the use of the vascular crusher gradient. It is well known that the vascular crusher gradient can be used to avoid the overestimation of absolute CBF values by eliminating intravascular signals in healthy subjects;[33] therefore, the vascular crusher gradient was also used in the present study. However, on the affected side, ATT is prolonged, and the labeled spin is retained in the blood vessel longer than on the unaffected side, and it may be possible that ASL-CBF was underestimated due to eliminating the intravascular signal to an extent more than necessary by using the crusher gradient. In addition, for both the unaffected and affected sides, the vascular crusher gradient is important when longer labeling settings are required, especially for short PLD data when labeled spins are retained in the intravascular space.[17] In

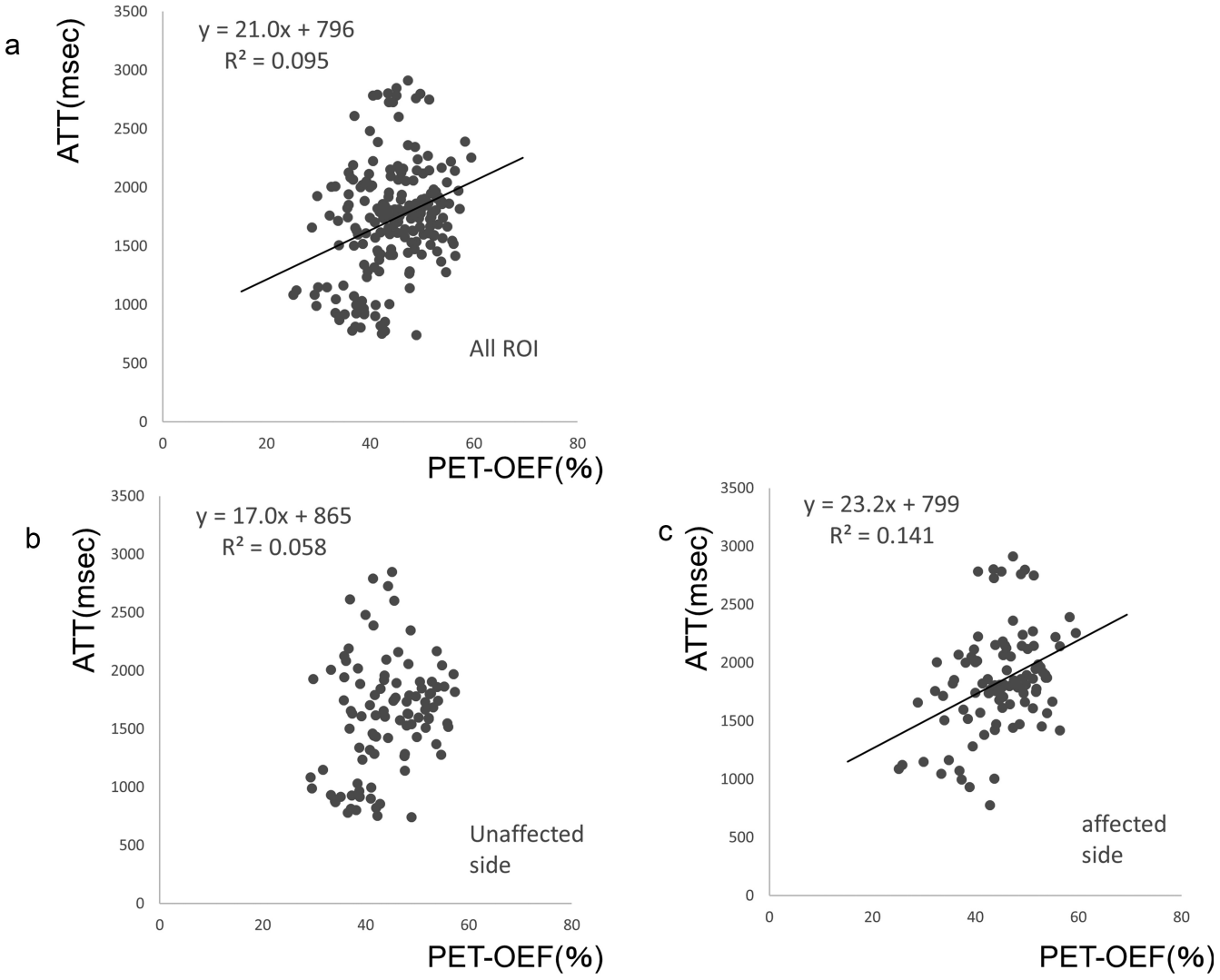

Fig. 5 Correlation between OEF and ATT. (**a**) Scatterplot showing the correlation of OEF and ATT values from both the affected and unaffected sides; (**b**) correlation of these values from only the hemisphere of the unaffected side; (**c**) correlation of these values from only the affected hemisphere. ATT, arterial transit time; OEF, oxygen extraction fraction.

the present study, a longer labeling period of 4s was used to increase the SNR of the perfusion signal, as well as of the vascular signal to the tissue signal, so that the vascular crusher gradient itself was indispensable for the imaging method of the present study.

Several studies have investigated the relationship between ATT and hemodynamic cerebral ischemia.[21,22] In the present study, ATT and the gold standard hemodynamic parameter, OEF, were compared for the first time. As shown in Fig. 5, the correlation between ATT and OEF was better when comparing only the affected side than when comparing both the unaffected side and the affected side. ATT varies even in normal subjects due to individual differences, and it is particularly affected by age.[34] According to classical autoregulation theory, OEF does not necessarily change in the normal perfusion state, and it increases only when compensating for decreased perfusion pressure or reduced CBF.[12] Therefore, a possible relationship between ATT and OEF should not be rejected just because the unaffected side did not show a significant correlation. The reason for the significant correlation between ASL-ATT and PET-OEF in the affected hemisphere can be inferred from the classical autoregulation theory reported by Powers:[12] cerebral artery stenosis or occlusion causes a decrease in perfusion pressure, a decrease in blood flow, an increase in OEF, and prolongation of ATT. Since both ATT and OEF are parameters that fluctuate when blood flow is decreased, they should be correlated. However, even in the presence of stenosis or occlusion, cerebral blood vessels form networks in the peripheral parenchyma, which compensate for the drop in perfusion pressure to some extent, as well as increasing

CBV, thereby compensating for blood flow. ATT is also expected to be extended in this condition. Therefore, it can be inferred that the increase in ATT includes both cases in which perfusion status worsens and cases in which perfusion is compensated for and blood flow does not worsen, and the correlation between ATT and OEF is weak. Previous studies have already reported that parameters similar to ASL-ATT have been compared with OEF. For example, Islam et al. reported a correlation between tracer delay time and OEF in PET CBF measurement, and they considered that delay time is closely correlated with hemodynamic impairment.[35] The nature of tracer delay time on PET is very similar to that of ATT in the ASL signal model. The tracer delay time is defined as the time difference between arterial tracer uptake as an arterial input function at the sampling site and tracer uptake of brain tissue. In contrast, in ASL, RF pulse irradiation is performed at the ICA trunk level, and the delay time to brain tissue is set to ATT. The fact that tracer delay time is correlated with OEF is very consistent with a significant correlation between ATT and OEF.

In addition, Gibbs et al. and Scuman et al. reported that MTT is an indicator of low cerebral perfusion pressure,[36,37] and Kamano et al. reported that there was a significant correlation between ATT and MTT, suggesting that ATT has the potential to detect hemodynamic impairment.[18] With chronic main cerebral artery stenosis or occlusion, the peripheral blood vessels dilate, and MTT prolongs to maintain blood flow according to the auto-regulation theory first reported by Powers.[12] MTT is the transit time of the microvascular network in the brain parenchyma, and ATT is the time to reach the brain parenchyma from the labeling plane of cervical blood vessels. As the transit time of peripheral blood vessels increases, it is inferred that the transit time from stenosis or occlusion to the periphery also increases. On the other hand, the reason why the correlation was weak may be variable prolongation of ATT due to the development of collateral circulation. Kamano et al. also considered the results of relative values to be more reliable than those of absolute values, and the reason for this may be that the ratio could normalize such variable prolongation of ATT.[18] In the present study as well, there was a weak but significant correlation between the ATT ratio and the MTT ratio.

Although ATT mapping has been suggested to reflect hemodynamic cerebral ischemia for some time, it does not correlate as strongly with OEF due to the effects of collateral circulation, making it difficult to replace all PET or SPECT studies with it. It is noteworthy, however, that ATT mapping can have some clinical value as an index of a compromised hemodynamic state; since ASL is completely non-invasive and repeatable, ASL-ATT might be useful when deciding whether to perform a PET or SPECT scan. Specifically, it was thought that we should consider how effective prolonged ATT would be in identifying a group of patients with hemodynamic cerebral ischemia who should undergo PET or SPECT. ATT map acquisition time was 2.5 min for the low-resolution pre-scan acquisition and short enough for use in routine clinical practice.

There are several potential limitations to this study. The ATT map cannot be calculated with the same resolution as the CBF map because the addition of the ASL signal increases the acquisition time. This problem may be partially solved by the acquisition of delay-encoded ASL,[38] which will allow for more efficient multi-PLD ASL acquisition. This patient population was not clinically homogeneous and was also limited in number; MRI and PET were not performed on the same day, but it should be noted that since chronic disease was being investigated, large hemodynamic changes due to the interval between examinations were not expected. Disorientation between PET and ASL CBF images has not yet been accurately assessed, but it may increase inter-case variability and decrease correlations between images. Even in the absence of these limitations, we believe that there would be little change in the correlation between PET-OEF and ASL-CBF, or in the need for ATT correction.

Conclusion

Low-resolution ATT correction may increase the accuracy of ASL-CBF measurements in patients with stenosis or occlusion of the cerebral arteries. In addition, ATT itself is a parameter that is affected by hemodynamic cerebral ischemia, and although it is difficult for it to completely substitute for PET-OEF, ATT might have a potential role in detecting compromised hemodynamic state.

Funding

This work was supported in part by a Grant-in-aid for Scientific Research (No. 21K07616) from the Japan Society for the Promotion of Science.

Conflicts of Interest

Naoyuki Takei is an employee of GE Healthcare Japan Corporation. The other authors have no potential conflicts of interest with respect to the research of this article.

References

1. Williams DS, Detre JA, Leigh JS, Koretsky AP. Magnetic resonance imaging of perfusion using spin inversion of arterial water. Proc Natl Acad Sci USA 1992; 89:212–216.
2. Detre JA, Leigh JS, Williams DS, Koretsky AP. Perfusion imaging. Magn Reson Med 1992; 23:37–45.
3. Alsop DC, Detre JA. Multisection cerebral blood flow MR imaging with continuous arterial spin labeling. Radiology 1998; 208:410–416.

4. Chalela JA, Alsop DC, Gonzalez-Atavales JB, Maldjian JA, Kasner SE, Detre JA. Magnetic resonance perfusion imaging in acute ischemic stroke using continuous arterial spin labeling. Stroke 2000; 31:680–687.
5. Detre JA, Alsop DC, Vives LR, Maccotta L, Teener JW, Raps EC, et al. Noninvasive MRI evaluation of cerebral blood flow in cerebrovascular disease. Neurology 1998; 50:633–641.
6. Wolf RL, Wang J, Wang S, et al. Grading of CNS neoplasms using continuous arterial spin labeled perfusion MR imaging at 3 Tesla. J Magn Reson Imaging 2005; 22:475–482.
7. Noguchi T, Yoshiura T, Hiwatashi A, et al. Perfusion imaging of brain tumors using arterial spin-labeling: correlation with histopathologic vascular density. AJNR Am J Neuroradiol 2008; 29:688–693.
8. Wu RH, Bruening R, Noachtar S, et al. MR measurement of regional relative cerebral blood volume in epilepsy. J Magn Reson Imaging 1999; 9:435–440.
9. Wolf RL, Wang J, Detre JA, Zager EL, Hurst RW. Arteriovenous shunt visualization in arteriovenous malformations with arterial spin-labeling MR imaging. AJNR Am J Neuroradiol 2008; 29:681–687.
10. Kodera T, Arai Y, Arishima H, et al. Evaluation of obliteration of arteriovenous malformations after stereotactic radiosurgery with Arterial Spin Labeling MR Imaging. Br J Neurosurg 2017; 31:641–647.
11. Kimura H, Kado H, Koshimoto Y, Tsuchida T, Yonekura Y, Itoh H. Multislice continuous arterial spin-labeled perfusion MRI in patients with chronic occlusive cerebrovascular disease: a correlative study with CO_2 PET validation. J Magn Reson Imaging 2005; 22:189–198.
12. Powers WJ, Press GA, Grubb RL Jr., Gado M, Raichle ME. The effect of hemodynamically significant carotid artery disease on the hemodynamic status of the cerebral circulation. Ann Intern Med 1987; 106:27–34.
13. Baron JC, Bousser MG, Rey A, Guillard A, Comar D, Castaigne P. Reversal of focal "misery-perfusion syndrome" by extra-intracranial arterial bypass in hemodynamic cerebral ischemia. A case study with 15O positron emission tomography. Stroke 1981; 12:454–459.
14. Yamauchi H, Fukuyama H, Nagahama Y, et al. Significance of increased oxygen extraction fraction in five-year prognosis of major cerebral arterial occlusive diseases. J Nucl Med 1999; 40:1992–1998.
15. Parkes LM, Tofts PS. Improved accuracy of human cerebral blood perfusion measurements using arterial spin labeling: Accounting for capillary water permeability. Magn Reson Med 2002; 48:27–41.
16. Tsujikawa T, Kimura H, Matsuda T, et al. Arterial transit time mapping obtained by pulsed continuous 3D ASL imaging with multiple post-label delay acquisitions: comparative study with PET-CBF in patients with chronic occlusive cerebrovascular disease. PLoS One 2016; 11:e0156005.
17. Dai W, Robson PM, Shankaranarayanan A, Alsop DC. Reduced resolution transit delay prescan for quantitative continuous arterial spin labeling perfusion imaging. Magn Reson Med 2012; 67:1252–1265.
18. Kamano H, Yoshiura T, Hiwatashi A, et al. Arterial spin labeling in patients with chronic cerebral artery steno-occlusive disease: correlation with 15O-PET. Acta Radiol 2013; 54:99–106.
19. Bokkers RPH, Bremmer JP, van Berckel BNM, et al. Arterial spin labeling perfusion MRI at multiple delay times: a correlative study with $H_2{}^{15}O$ positron emission tomography in patients with symptomatic carotid artery occlusion. J Cereb Blood Flow Metab 2010; 30:222–229.
20. Dai W, Robson PM, Shankaranarayanan A, Alsop DC. Reduced resolution transit delay prescan for quantitative continuous arterial spin labeling perfusion imaging. Magn Reson Med 2012; 67:1252–1265.
21. Bokkers RPH, van Laar PJ, van de Ven KCC, Kapelle LJ, Klijn CJ, Hendrikse J. Arterial spin-labeling MR imaging measurements of timing parameters in patients with a carotid artery occlusion. AJNR Am J Neuroradiol 2008; 29:1698–1703.
22. MacIntosh BJ, Lindsay AC, Kylintireas I, et al. Multiple inflow pulsed arterial spin-labeling reveals delays in the arterial arrival time in minor stroke and transient ischemic attack. AJNR Am J Neuroradiol 2010; 31:1892–1894.
23. Ferguson GG, Eliasziw M, Barr HWK, et al. The North American Symptomatic Carotid Endarterectomy Trial (NASCET): surgical results in 1415 patients. Stroke 1999; 30:1751–1758.
24. Ishida S, Kimura H, Isozaki M, et al. Robust arterial transit time and cerebral blood flow estimation using combined acquisition of Hadamard-encoded multi-delay and long-labeled long-delay pseudo-continuous arterial spin labeling: a simulation and in vivo study. NMR Biomed 2020; 33:e4319.
25. DeGrado TR, Turkington TG, Williams JJ, Stearns CW, Hoffman JM, Coleman RE. Performance characteristics of a whole-body PET scanner. J Nucl Med 1994; 35:1398–1406.
26. Isozaki M, Kiyono Y, Arai Y, et al. Feasibility of ^{62}Gu-ATSM PET for evaluation of brain ischemia and misery perfusion in patients with cerebrovascular disease. Eur J Nucl Med Mol Imaging 2011; 38:1075–1082.
27. Okazawa H, Tsuchida T, Kobayashi M, et al. Can reductions in baseline CBF and vasoreactivity detect misery perfusion in chronic cerebrovascular disease?. Eur J Nucl Med Mol Imaging 2007; 34:121–129.
28. Mintun MA, Raichle ME, Martin WRW, Herscovitch P. Brain oxygen utilization measured with 0–15 radiotracers and positron emission tomography. J Nucl Med 1984; 25:177–187.
29. Zierler KL. Theoretical basis of indicator-dilution methods for measuring flow and volume. Circ Res 1962; 10:393–407.
30. Mutsaerts HJ, van Dalen JW, Heijtel DF, et al. Cerebral perfusion measurements in elderly with hypertension using arterial spin labeling. PLoS One 2015; 10:e0133717.
31. Ogura T, Hida K, Masuzuka T, Saito H, Minoshima S, Nishikawa K. An automated ROI setting method using NEUROSTAT on cerebral blood flow SPECT. Ann Nucl Med 2009; 23:33–41.
32. Mukaka MM. Aguide to appropriate use of Correlation coefficient in medical research. Malawi Med J 2012; 24:69–71.
33. Ye FQ, Mattay VS, Jezzard P, Frank JA, Weinberger DR, McLaughlin AC. Correction for vascular artifacts in cerebral blood flow values measured by using arterial spin tagging techniques. Magn Reson Med 1997; 37:226–235.
34. Fujiwara Y, Matsuda T, Kanamoto M, et al. Comparison of long-labeled pseudo-continuous arterial spin labeling (ASL)

features between young and elderly adults: special reference to parameter selection. Acta Radiol 2017; 58:84–90.
35. Islam MM, Tsujikawa T, Mori T, Kiyono Y, Okazawa H. Pixel-by-pixel precise delay correction for measurement of cerebral hemodynamic parameters in $H_2{}^{15}O$ PET study. Ann Nucl Med 2017; 31:283–294.
36. Gibbs JM, Wise RJ, Leenders KL, Jones T. Evaluation of cerebral perfusion reserve in patients with carotid-artery occlusion. Lancet 1984; 1:310–314.
37. Schumann P, Touzani O, Young AR, Morello R, Baron JC, MacKenzie ET. Evaluation of the ratio of cerebral blood flow to cerebral blood volume as an index of local cerebral perfusion pressure. Brain 1998; 121:1369–1379.
38. Dai W, Shankaranarayanan A, Alsop DC. Volumetric measurement of perfusion and arterial transit delay using hadamard encoded continuous arterial spin labeling. Magn Reson Med 2013; 69:1014–1022.